UNITED STATES DEPARTMENT OF THE INTERIOR
GEOLOGICAL SURVEY

Compilation of sample preparation and analytical methods and results of chemical, isotopic, and fluid inclusion analyses, Rodalquilar gold-alunite deposit, Spain

by

Arribas Jr., Antonio[1,5]
Cunningham, Charles G.[2]
McKee, Edwin H.[3]
Rye, Robert O.[4]
Rytuba, James J.[3]
Tosdal, Richard M.[3]
Wasserman, Michael D.[4]
Aoki, Masahiro[5]

Open-File Report 95-221

1) Department of Geology, University of Michigan, Ann Arbor, Michigan 48109
2) U.S. Geological Survey, National Center, Reston, Virginia 22092
3) U.S. Geological Survey, 345 Middlefield Road, Menlo Park, California 84025
4) U.S. Geological Survey, Federal Center, Denver, Colorado 80225
5) Geological Survey of Japan, 1-1-3 Higashi, Tsukuba, 305 Japan

TABLE OF CONTENTS

INTRODUCTION

Understanding the evolution of the calderas and origin of gold-alunite deposit of Rodalquilar, southeastern Spain (Figs. 1 and 2), were the objectives of a U.S.-Spain cooperative project financially supported by the U.S.-Spain Joint Committee for Scientific and Technological Cooperation. Results of studies on the calderas and geologic setting of the gold-alunite metal deposit were published by Cunningham et al. (1990) and Rytuba et al. (1990). The detailed study of the ore deposits and geochemistry of wall rock alteration and ore mineralization was a multidisciplinary effort and the subject of a Ph.D. thesis by Antonio Arribas Jr. at the University of Michigan (Arribas, 1992). The main interpretations and conclusions of these studies have been integrated in a summary paper by Arribas et al. (1995). However, due to journal space limitations, the results of individual chemical, isotopic and fluid inclusion analyses, as well as details of sample preparation and analytical methods, were not reported. Those data are compiled in this open-file report.

SAMPLE PREPARATION AND ANALYTICAL METHODS

Mineral separation

Considerable effort was expended to obtain pure (≥95%) mineral separates for isotopic analyses. Even then, samples of illite and kaolinite prepared by centrifugation may contain up to 25% total of quartz, pyrophyllite, alunite, or chlorite. Illite and kaolinite separates were extracted, respectively, from drill core and surface samples of altered intracaldera tuffs by selecting the grain size fraction (e.g., <0.2 μm, 1 to 0.2 μm) that contained the smallest amounts of contaminant phases (e.g., chlorite, pyrophyllite). About 100 to 200 g of core, depending on the relative proportion of clays, were hand-crushed in a mortar, and sieved (<1 mm) to separate large quartz phenocrysts and silicified clots. Fine-grained minerals were dissagregated by using an ultrasonic probe and separated by settling in a water column followed by centrifuging (see Appendix A in Wasserman et al., 1992). Stage 1 alunite was sampled from the advanced argillic core of the Cinto center (Fig. 3) and separated by microdrilling from thick (~1 mm) sections of rock. Stage 2 alunite was prepared by powdering selected chips of the

texturally most uniform material from hand specimens of alunite veinlets or open space fillings.

K-Ar dating

K-Ar analyses on illite and alunite were made at the U.S. Geological Survey, Menlo Park, laboratories using standard isotope-dilution procedures (Dalrymple and Lanphere, 1969). K_2O concentration was determined by lithium metaborate flux fusion-flame photometry (Ingamells, 1970), and Ar isotope analyses were performed using a 60° sector, 15.2 cm-radius, Nier-type mass spectrometer operated in the static mode of a 5-collector system for simultaneous measurement of the isotopic ratios (Stacey et al., 1981). A single $^{40}Ar/^{39}Ar$ determination of Stage 2 alunite followed handling techniques described by Dalrymple and Lanphere (1971). The sample was irradiated in the U.S. Geological Survey TRIGA reactor for a period of 20 hr at a power of 1 MW. Irradiation flux was monitored by use of the SB-3 biotite standard and correction for calcium- and potassium-derived isotopes followed procedures described by Dalrymple and Lanphere (1971).

Fluid inclusions

Heating and freezing measurements were made using a Fluid Inc. stage at the U.S. Geological Survey, Reston. The number of measurements during each run varied between 1 and 8. Analytical precision is better than ± 2°C for homogenization temperatures and better than ± 0.1°C for the final-melting temperatures of ice. The stage was calibrated using synthetic fluid inclusions (Sterner and Bodnar, 1984) and various standards of known melting point. Salinities were calculated using data of Hall et al. (1988) for the NaCl-KCl-H_2O system.

Stable isotopes

Sulfur, O, and H isotope compositions were measured at the laboratories of the U.S. Geological Survey in Denver, Colorado, and are reported as δ values, in per mil (‰) relative to the Canyon Diablo troilite (for S) and SMOW (for O and H) standards. Sulfur was extracted from pure sulfides as SO_2 by combustion with cuprous oxide (1 mg of CuO per micromole of converted SO_2) for 10 minutes at 1025°C. Sulfur in chalcedonic-quartz gold ore was extracted prior to combustion by digestion in $CrCl_2$-HCl and precipitation as AgS_2 (Zhabina and Volkov, 1978). In this research, 50-100 mg of sulfide-bearing samples were dissolved for 1 to 2 hours

at 80°C in a solution of 25 ml 6N HCl–25 ml 0.5N $CrCl_2$–5 ml ethanol. The resulting H_2S gas was passed in a nitrogen stream through a solution of 5% $AgNO_3$–10% NH_4OH, where fine-grained Ag_2S precipitated. The black powdery precipitate was then recovered onto 0.45 μm Millipore filters. The Kiba-reagent technique (Sasaki et al., 1979) was used to separate S from whole rock samples.

For isotopic analysis of sulfur and sulfate-oxygen, barite was selectively dissolved in a heated solution of 5% Na_2CO_3, and alunite and jarosite in a heated solution of 0.5 N NaOH (Wasserman et al., 1992). The sulfate in solution was then precipitated as $BaSO_4$ and analyzed for $\delta^{34}S$ and $\delta^{18}O_{SO4}$, respectively, using the direct thermal decomposition (Holt and Engelkemeir, 1970) and graphite reduction (Sakai and Krouse, 1971) techniques. $\delta^{18}O_{OH}$ analyses of alunite were performed using a total fluorination method described in detail in Wasserman et al. (1992). $\delta^{18}O_{OH}$ is calculated from a mass balance equation which includes terms for the isotopic composition of bulk oxygen produced by fluorination of alunite ($\delta^{18}O_{BrF5}$), the fractionation of oxygen during fluorination of sulfate ($\Delta^{18}O_{SO4(Gr\text{-}Fl)}$), $\delta^{18}O_{SO4}$, and the molar ratios of oxygen liberated from hydroxil and sulfate in alunite. Oxygen isotope ratios in silicates (e.g., quartz, illite, kaolinite) and silicate rock were analyzed by conventional procedures (Clayton and Mayeda, 1963).

Determination of δD values were performed using reduction with uranium (Friedman, 1953) on water derived from alunite, illite, and kaolinite by inductively coupled thermal decomposition. Production of sulfuric acid and formation of potassium±sodium oxides during δD analyses of alunite was minimized by step heating to a temperature only high enough to just completely dehydrate the mineral (Wasserman et al., 1992).

Measurement of H/D and $^{34}S/^{32}S$ values were performed on modified Nuclide 6-60 RMS mass spectrometers. Oxygen isotope ratios were measured using a Finnigan MAT 251 triple-cup mass spectrometer. The $\delta^{34}S$ values are reproducible to ± 0.15 per mil except for whole rock samples prepared using the Kiba technique that are reproducible to ± 0.6 per mil. The analytical uncertainties (1σ) of $\delta^{18}O_{SO4}$, $\delta^{18}O_{OH}$, $\delta^{18}O$, and δD, respectively are ± 0.15, ± 0.3, ±0.1, and ± 3 per mil.

Radiogenic isotopes

For lead and strontium isotope analyses, alunite and whole rock samples were dissolved in HF-HCl. Lead was separated using HBr on anion exchange columns, and strontium was collected from the same columns, redissolved in HCl, and

separated using HCl cation exchange columns. Aliquots of the strontium- and lead- bearing solutions were deposited on molybdenum and rhenium filaments, respectively, and analyzed on a Finnigan MAT 262 multiple collector mass spectrometer at the U.S. Geological Survey in Menlo Park, California (analytical procedures modified from Wooden et al., 1992). Measured lead-isotope ratios were corrected for 0.125 percent per atomic-mass unit fractionation, based on replicate analyses of NBS 981 standard. Laboratory procedural blanks were 2 ng lead or less and the precision of isotopic measurements better than 0.05 percent at the 2-sigma confidence level. Lead isotope ratios are reproducible to ± 0.08, ± 0.10, and ± 0.14 percent (2σ), respectively, for $^{206}Pb/^{204}Pb$, $^{207}Pb/^{204}Pb$, and $^{208}Pb/^{204}Pb$. Strontium isotope ratios were normalized to $^{86}Sr/^{88}Sr = 0.1194$, and are reproducible to ± 0.1 percent.

REFERENCES

Arribas, A. Jr., 1992, Geology and geochemistry of the Rodalquilar gold-alunite deposit; relationship to other hydrothermal ore deposits in southeastern Spain: Unpub. Ph.D. thesis, Univ. Michigan, 320 p.

Arribas, A. Jr., and Tosdal, R.T., 1994, Isotopic composition of Pb in ore deposits of the Betic Cordillera, Spain: Origin and relationship to other European deposits: Economic Geology, v. 89, p. 1074–1093.

Arribas, A. Jr., Cunningham, C. G., Rytuba, J. J., Rye, R. O., Kelly, W.C., McKee, E. H., Podwysocky, M. H., and Tosdal, R. M., 1995, Geology, geochronology, fluid inclusions, and isotope geochemistry of the Rodalquilar Au-alunite deposit, Spain: Economic Geology, v. 90 (in press)

Bird, M. I., Andrew, A. S., Chivas, A. R., and Lock, D. E., 1989, An isotopic study of surficial alunite in Australia 1: Hydrogen and sulfur isotopes: Geochimica et Cosmochimica Acta, v. 53, p. 3223–3237.

Clayton, R. N. and Mayeda, T. K., 1963, The use of bromine pentafluoride in the extraction of oxygen from oxides and silicates for isotopic analysis: Geochimica et Cosmochimica Acta, v. 27, p. 43–52.

Cunningham, C. G., Arribas, A., Jr., Rytuba, J. J., and Arribas, A., 1990, Mineralized and unmineralized calderas in Spain; Part I, evolution of the Los Frailes caldera: Mineralium Deposita, v. 25 (Suppl), p. S21–S28.

Dalrymple, G. B., and Lanphere, M. A., 1969, Potassium-Argon dating: San Francisco, W.H. Freeman Company, 258 p.

Dalrymple, G. B., and Lanphere, M. A., 1971, $^{40}Ar/^{39}Ar$ technique of K-Ar dating: A comparison with the conventional technique: Earth and Planetary Science Letters, v. 12, p. 300–308.

Eslinger, E. V., and Savin, S. M., 1973, Mineralogy and oxygen isotope geochemistry of the hydrothermally altered rocks of the Ohaki-Broadlands, New Zealand geothermal area: America Journal of Science, v. 273, p. 240–270.

Eslinger, E. V., Savin, S. M., and Yeh, H., 1979, Oxygen isotope geothermometry of diagenetically altered shales: SEPM Special Publication No. 26, March, 1979, p. 113–124.

Friedman, I., 1953, Deuterium content of natural waters and other substances: Geochimica et Cosmochimica Acta, v. 4, p. 89–103.

Hall, D. L., Sterner, S. M., and Bodnar, R. J., 1988, Freezing point depression of NaCl-KCl-H_2O solutions: Economic Geology, v. 83, p. 197–202.

Holland, H. D., and Malinin, S. D, 1979, The solubility and occurrence of non-ore minerals, *in* Barnes, H. L., ed., Geochemistry of hydrothermal ore deposits: New York, Wiley Intersci., p. 461–508.

Holt, B. D. and Engelkemeir, A. G., 1970, The thermal decomposition of barium sulfate to sulfur dioxide for mass spectrometer analysis: Analytical Chemistry, v. 42, p. 1451–1453.

Ingamells, C. O., 1970, Lithium metaborate flux in silicate analysis: Analytica Chimica Acta, v. 52, p. 323–334.

Kita, I., Taguchi, S., and Matsubaya, O., 1985, Oxygen isotope fractionations between amorphous silica and water at 34-93°C: Nature, v. 314, p. 63–64.

Marumo, K., Nagasawa, K., and Kuroda, Y., 1980, Mineralogy and hydrogen isotope geochemistry of clay minerals in the Ohnuma geothermal area, northeastern Japan: Earth and Planetary Science Letters, v. 47, p. 255-262.

Matsuhisa, Y., Goldsmith, J. R., and Clayton, R. N., (1979), Oxygen isotopic fractionation in the system quartz-albite-anorthite-water: Geochimica et Cosmochimica Acta, v. 43, p. 1131–1140.

Ohmoto, H., and Lasaga, A. C., 1982, Kinetics of reactions between aqueous sulfates and sulfies in hydrothermal systems: Geochimica et Cosmichimica Acta, v. 46, p. 1727–1745.

Ohmoto, H., and Rye, R. O., 1979, Isotopes of sulfur and carbon, in Barnes, H. L., ed., Geochemistry of hydrothermal ore deposits: New York, Wiley Intersci., p. 509–567.

Rytuba, J. J., Arribas, A., Jr., Cunningham, C. G., McKee, E. H., Podwysocki, M. H., Smith, J. G., Kelly, W. C., and Arribas, A., 1990, Mineralized and unmineralized calderas in Spain; Part II, evolution of the Rodalquilar caldera complex and associated gold-alunite deposits, Mineralium Deposita, v. 25 (Suppl), p. S29–S35.

Sakai, H., and Krouse, H. R., 1971, Elimination of memory effects in $^{18}O/^{16}O$ determinations in sulphates: Earth and Planetary Science Letters, v. 11, p. 369–373.

Sasaki, A., Arikawa, Y., and Folinsbee, R. E., 1979, Kiba reagent method of sulfur extraction applied to isotope work: Geological Survey of Japan Bulletin, v. 30, p. 241–245.

Savin, S. M., and Lee, 1988, Isotopic studies of phyllosilicates; Reviews in Mineralogy, v. 19, p. 189–219.

Stacey, J. S., Sherrill, N. D., Dalrymple, G. B., Lanphere, M. A., and Carpenter, N. V., 1981, A five-collector system for the simultaneous measurement or argon isotopic ratios in a static mass spectometer: International Journal of Mass Spectrometry and Ion Physics, v. 39, p. 167–180.

Sterner, S. M., and Bodnar, R. J., 1984, Synthetic fluid inclusions in natural quartz I. Compositional types synthesized and applications to experimental geochemistry: Geochimica et Cosmochimica Acta, v. 48, p. 2659–2668.

Stoffregen, R.E., Rye, R.O., and Wasserman, D.M., 1994, Experimental studies of alunite I: ^{18}O-^{16}O and D-H fractionations factors between alunite and water at 250-450°C: Geochimica et Cosmochimica Acta, v. 58, p. 903–916.

Ueda, A., and Sakai, H., 1983, Simultaneous determination of the concentration and isotope ratio of sulfate-and sulfide-sulfur and carbonate-carbon in geological samples. Geochemical Journal, v. 17, p. 185–196.

Wasserman, M.D., Rye, R.O., Bethke, P.M., and Arribas, A. Jr, 1992, Methods for separation and total stable isotope analysis of alunite: U.S. Geol. Survey Open-File Report 92-9, 20 p.

Wooden, J. L., Czamanske, G. K., Bouse, R. M., Likhachev, A.P., Kunilov, V. E., and Lyul'lp, V., 1992, Pb isotope data indicate a complex mantle origin for the Noril'sk Talnakh ores, Siberia: Economic Geology, v. 87, p. 1153–1165.

Zhabina, N. N., and Volkov, I. I., 1978, A method of determination of various sulfur compounds in the sea sediments and rocks: in W.E. Krumbein (ed.), Environmental biogeochemistry and geomicrobiology, Vol. 3: Methods, metals and assessment: Ann Arbor, Ann Arbor Science Pub., p. 735-746.

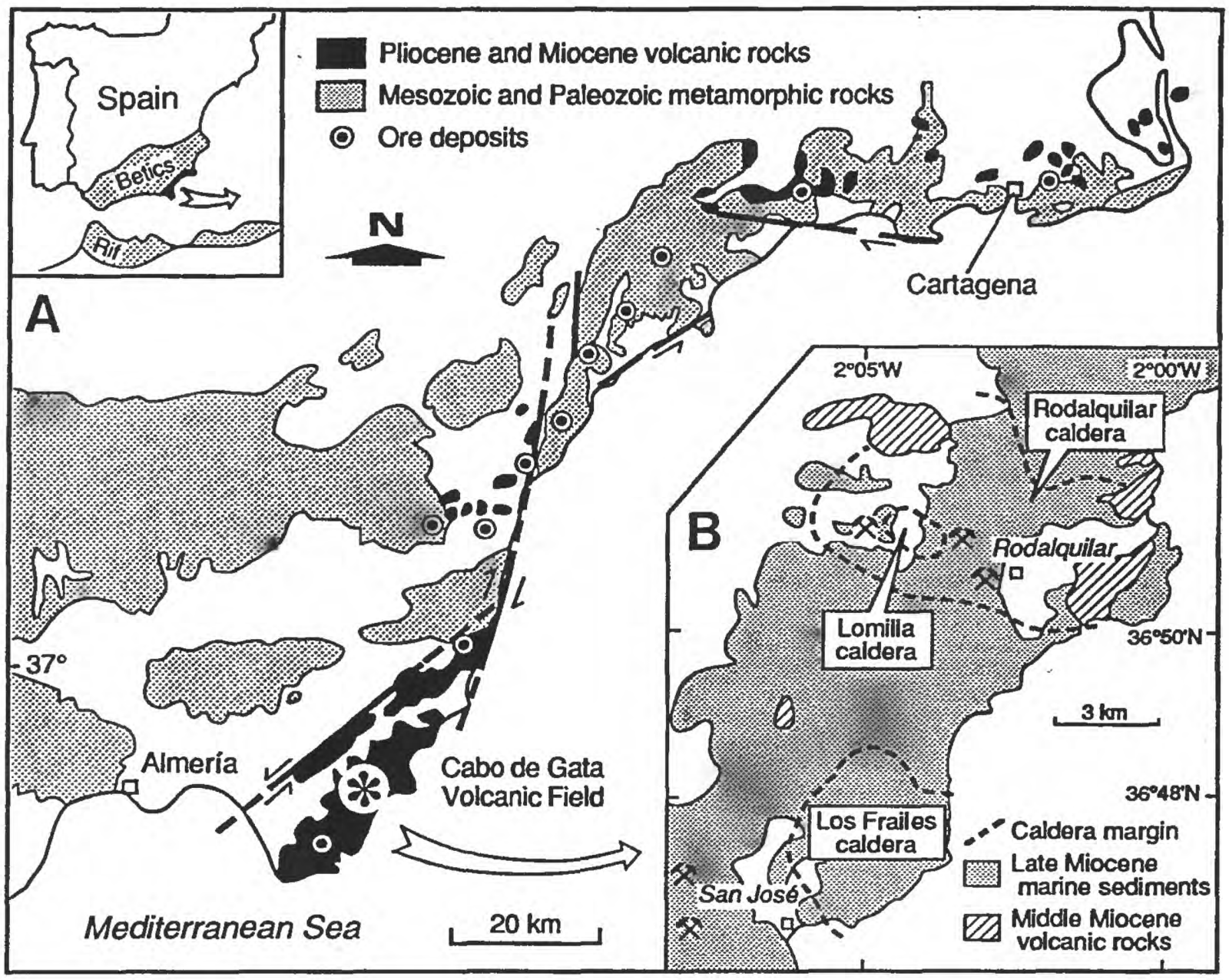

Fig. 1. Location of the Rodalquilar gold-alunite deposit within the Cabo de Gata volcanic field, Betic Cordillera (inset), southeastern Spain. B. Index map of the central part of the volcanic field with indication of the Los Frailes, Rodalquilar and Lomilla caldera margins.

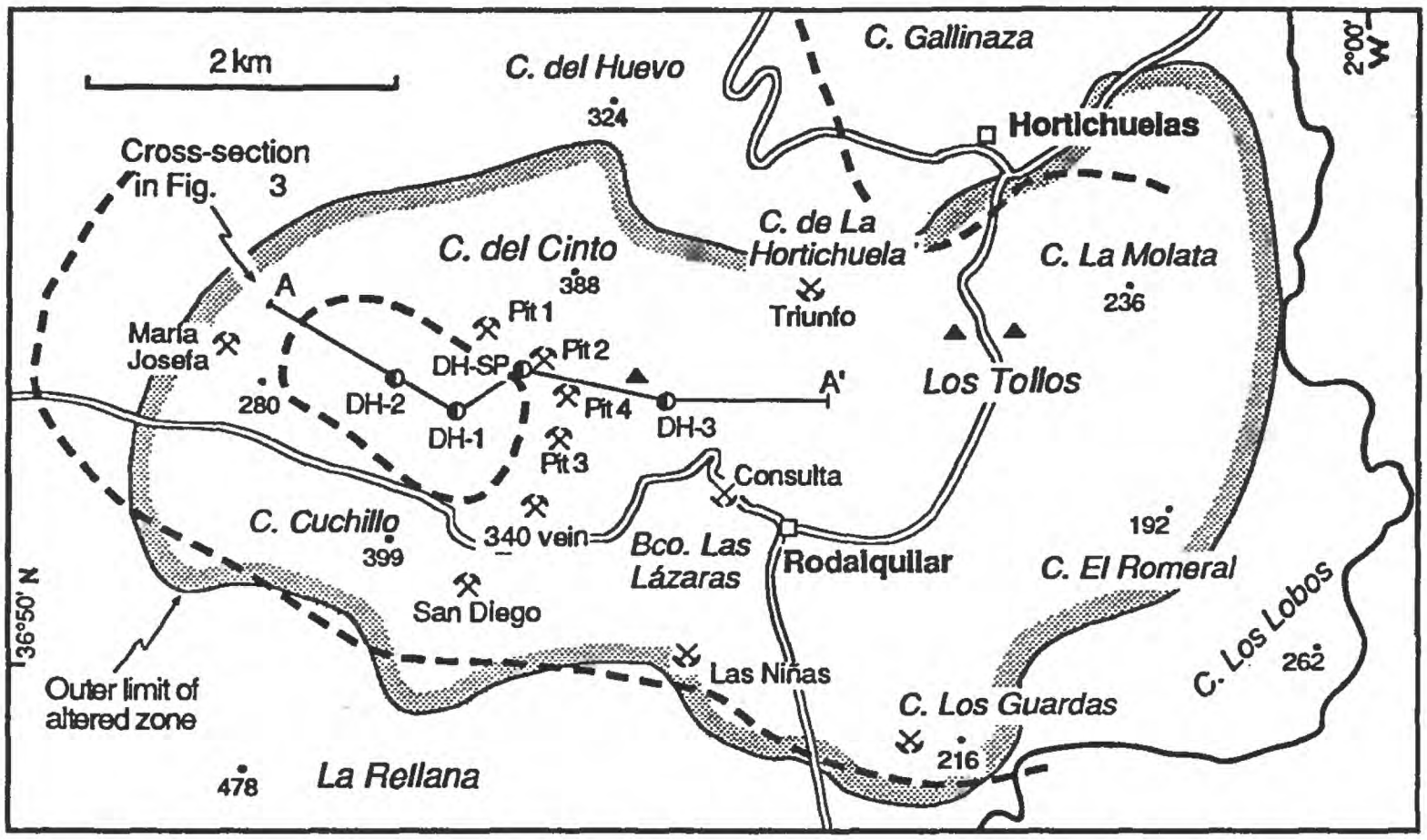

Fig. 2. Map of the Rodalquilar caldera showing location of ore deposits, the extent of the zone of altered rocks, and geographic features mentioned in the data tables. Spanish names and abbreviations as follows: Cerro (C) = hill, Barranco (Bco) = ravine.

A. Lithology

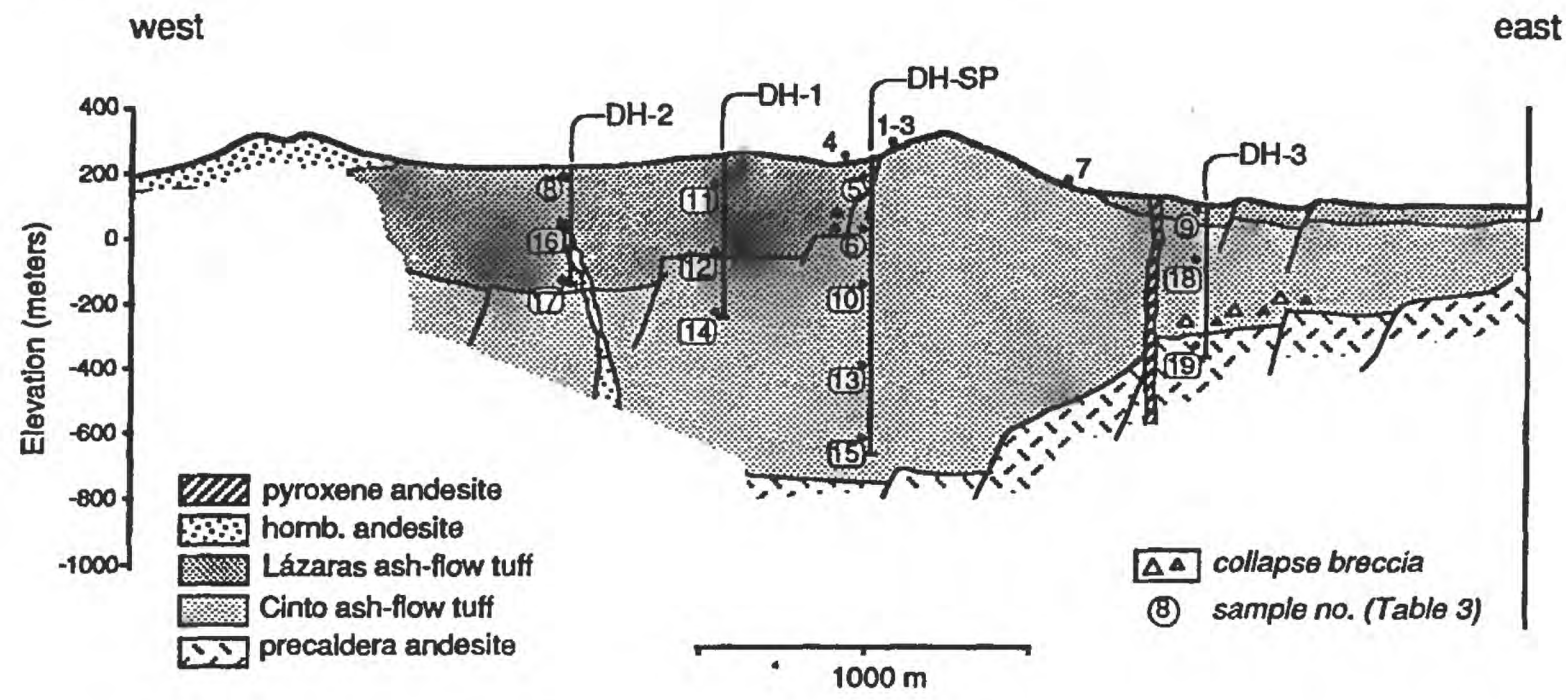

B. Hydrothermal alteration and mineralization

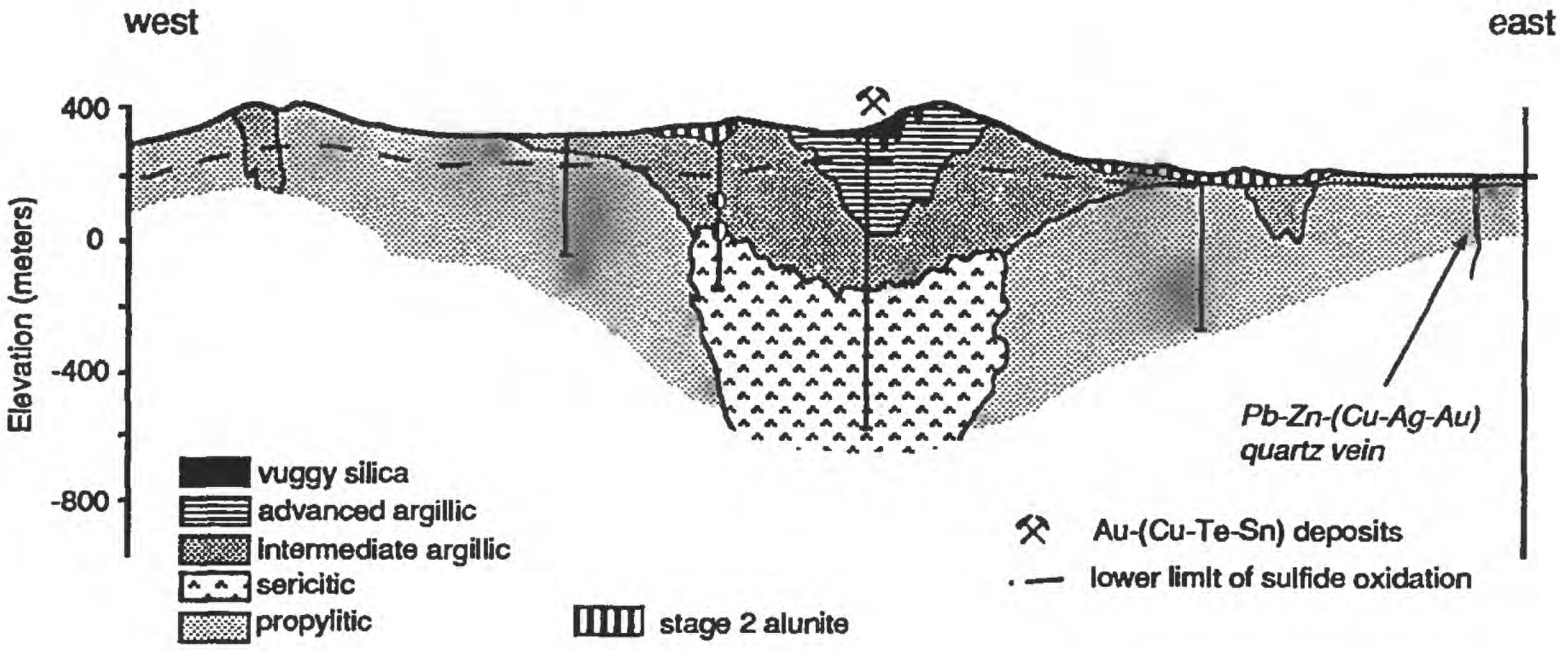

Fig. 3. Schematic cross-sections showing lithology (A) and hydrothermal alteration and location of ore deposits (B) in the Rodalquilar and Lomilla calderas. Numbers in (A) correspond to sample numbers in Table 3.

Table 1. Chemical Composition of Volcanic Rocks Related to the Rodalquilar Gold Deposit, SE Spain

Sample No.*	88BA17	86189	86A43	87A344	87A372	87ALAZ	HPOR	86A186-1	87ALOB
SiO_2 (wt %)	59.50	61.10	64.20	67.20	67.30	61.20	60.40	62.10	59.00
Al_2O_3	15.50	15.70	15.10	14.40	14.60	13.40	15.00	16.20	17.80
Fe_2O_3§	5.89	5.77	4.35	2.37	3.48	4.43	6.85	5.97	6.79
MgO	2.84	2.13	0.50	1.44	0.62	2.72	4.50	3.12	3.55
CaO	6.26	5.33	0.92	2.97	3.23	5.20	7.79	5.72	7.82
Na_2O	2.01	1.95	0.59	2.71	2.41	1.96	2.29	2.58	2.04
K_2O	3.46	4.25	11.10	2.71	3.14	2.07	1.52	2.03	1.23
TiO_2	0.60	0.62	0.46	0.25	0.44	0.42	0.53	0.53	0.84
P_2O_5	0.12	0.12	0.05	0.09	0.11	0.10	0.10	0.12	0.14
MnO	0.17	0.18	0.08	0.05	0.02	0.12	0.12	0.11	0.11
LOI 925°C	2.94	2.32	2.55	5.97	3.88	7.91	1.31	1.87	0.92
Total	99.29	99.47	99.90	100.16	99.23	99.53	100.41	100.35	100.24
Zn (ppm)	122	178	32	42	720	54	60	310	70
Rb	188	235	555	196	134	116	52	82	62
Sr	210	200	62	170	146	70	130	154	225
Y	20	24	36	24	22	18	12	22	28
Zr	100	114	122	122	114	106	78	98	180
Nb	—	—	—	—	—	—	—	—	13
Ba	385	920	640	265	295	184	155	300	405
Rb/Sr	*0.90*	*1.18*	*8.96*	*1.15*	*0.92*	*1.66*	*0.4*	*0.53*	*0.28*
La	17.4	17.5	29.3	34.9	27.6	19.4	15.5	16.6	29.5
Ce	32.5	36.8	55.4	68.2	48.7	37.9	32.8	33.0	54.0
Nd	17.1	16.6	24.3	31.5	22.1	18.5	12.3	15.2	28.7
Sm	3.26	3.59	4.20	4.73	4.29	3.41	2.69	3.29	5.34
Eu	0.65	0.96	0.88	0.80	0.67	0.68	0.76	0.95	1.18
Dy	3.57	3.01	3.62	3.35	3.53	2.63	3.41	3.33	4.90
Yb	1.69	1.66	1.82	2.09	1.94	1.62	1.51	1.80	2.66
Lu	0.29	0.31	0.27	0.36	0.33	0.29	0.24	0.28	0.43
Lat. North	02°02'30"	02°01'50"	02°03'20"	02°02'30"	02°03'20"	02°03'00"	02°03'05"	02°03'35"	02°02'30"
Long. East	36°49'35"	36°50'00"	36°49'50"	36°52'20"	36°52'10"	36°50'55"	36°52'30"	36°51'17"	36°50'20"

* Samples: See Figure 2 for location of geographic features within the Rodalquilar caldera

- 88BA17 Precaldera andesite flow in southern margin of the Rodalquilar caldera
- 86A189 Precaldera andesite in La Higuera
- 86A43 Outflow facies (unit No. 6) of Cinto ash-flow tuff, La Rellana
- 87A344 Caldera-fill facies of Cinto ash-flow tuff, southeast of Cerro del Huevo
- 87A372 Rhyolite dome in Cerro del Cinto (propylitically altered)
- 87ALAZ Lázaras ash-flow tuff in Barranco de las Lázaras (propylitically altered)
- HPOR Hornblende andesite flow in Cerro del Huevo
- 86A186-1 Hornblende andesite plug in open pit 3 Cerro del Cinto
- 87ALOB Postcaldera pyroxene andesite in Cerro de los Lobos

— = not detected (Nb < 10 ppm, Gd <4.5 ppm); Fe_2O_3§ = total iron as Fe_2O_3

Major elements analyzed by wavelength-dispersive X-ray fluorescence (USGS, Denver; D.F. Siems and J.E. Taggart, analysts); Zn, Rb, Sr, Y, Zr, Nb, Ba analyzed by energy-dispersive XRF (USGS, Menlo Park); rare-earth elements analyzed by instrumental neutron activation (Phoenix Memorial Laboratory, University of Michigan, Ann Arbor)

Table 2. K-Ar and ^{40}Ar-^{39}Ar Data for Samples of Alteration Minerals from the Rodalquilar Deposit

Sample no.	Location (elevation, m a.s.l.)	Mineral concentrated	Other minerals in concentrate[1]	K_2O (%)	$^{40}Ar^*$ (mole/g)	$^{40}Ar^*/\Sigma^{40}Ar$	Age ± 1 sd (Ma)
87A21	DH-1, 367 m (-110)	Illite (<2 μm)	Pyrophyllite	8.10	1.262×10^{-10}	64	10.8 ± 0.6
87A10	DH-1, 441 m (-190)	Illite (<2 μm)	Chlorite (25%), quartz (10%)	5.97	9.286×10^{-11}	63	10.8 ± 0.3
87A14	DH-1, 480 m (-230)	Illite (<2 μm)	Quartz	8.49	1.358×10^{-10}	34	11.1 ± 0.7
87A125	DH-SP, 760 m (-530)	Illite (<2 μm)	Chlorite (15%), quartz	7.29	9.881×10^{-11}	14	9.4 ± 0.8
87A150	Cinto pit no. 1, 290-m bench	Alunite stg. 1	Quartz, hematite	8.44	1.236×10^{-10}	24	10.1 ± 0.6
87A111	DH-SP, 130 m (100)	Alunite stg. 1	Zunyite (10%), quartz, pyrite	4.89	7.326×10^{-11}	12	10.4 ± 0.6
86A32	Cinto pit no. 3, 290-m bench	Alunite stg. 2	Kaolinite (~5%), quartz	10.08	4.362×10^{-11}	8.4	3.0 ± 0.2
87A373	SW flank of Cerro Cinto (170)	Alunite stg. 2	None	10.49	4.663×10^{-11}	21	3.1 ± 0.1
87A380	NW flank of Cerro Cinto (290)	Alunite stg. 2	Quartz, kaolinite	8.21	4.089×10^{-11}	15	3.5 ± 0.2
87A97	150 m east of 340 vein (200)	Alunite stg. 2	Quartz	10.56	5.756×10^{-11}	39	3.8 ± 0.1

$^{40}Ar/^{39}Ar$

Sample no.	Location (elevation, m a.s.l.)	Mineral concentrated	Other minerals in concentrate	$^{40}Ar/^{39}Ar$	$^{37}Ar/^{39}Ar$ ($\times 10^{-3}$)	$^{36}Ar/^{39}Ar$ ($\times 10^{-3}$)	$\%^{40}Ar^*$	$\%^{39}Ar^{Ca}$ ($\times 10^{-4}$)	$\%^{36}Ar^{Ca}$ ($\times 10^{-2}$)	J	Age ± 1sd (Ma)
87A67	DH-1, 180 m (70)	Alunite stg. 2	Quartz, illite-smectite, kaolinite	1.36289	6.68487	3.6374	20.7	4.5	4.9	0.0058	2.95 ± 0.07

See Figure 2 for location of mines and drill holes within the Rodalquilar caldera complex

[1] Less than 3% of each mineral, except where noted, based on powder X-ray diffraction

Table 3. Chemical Composition of Altered Rocks Related to the Rodalquilar Gold Deposit, Spain

	Silicic zone (Vuggy silica)			Advanced argillic zone			Intermediate argillic zone (near-surface)		
Sample No.*	87A230	87A171a	87A285	87A169	SRT60	SRT185	87A209	S2-20	S3-27
Location¶	(1)	(2)	(3)	(4)	(5)	(6)	(7)	(8)	(9)
SiO_2 (wt %)	95.0	89.7	93.4	82.0	83.4	70.4	65.1	67.4	67.7
Al_2O_3	1.19	2.25	0.78	6.84	6.78	16.8	15.3	19.0	18.7
Fe_2O_3§	0.85	2.37	2.58	0.98	3.21	2.53	3.46	0.25	4.17
MgO	<0.10	<0.10	<0.10	<0.10	<0.10	0.16	1.94	0.64	0.32
CaO	0.03	0.05	<0.02	0.03	<0.02	0.1	0.28	0.20	0.05
Na_2O	<0.15	0.19	0.17	0.31	<0.15	0.32	2.67	1.76	<0.15
K_2O	0.12	0.4	0.21	0.99	0.35	0.69	6.40	4.32	1.91
TiO_2	0.38	0.38	0.38	0.40	0.41	0.42	0.47	0.58	0.62
P_2O_5	0.09	0.14	<0.05	0.12	<0.05	0.16	0.08	<0.05	<0.05
MnO	<0.02	<0.02	<0.02	<0.02	<0.02	<0.02	0.12	<0.02	<0.02
LOI 925°C	1.22	3.16	2.21	7.48	4.62	7.66	3.19	5.02	6.59
Total	99.15	98.76	99.92	99.27	99.11	99.26	99.01	99.24	100.28
Cu (ppm)	<20	<20	50	<20	134	<20	<20	32	<20
Zn	<20	<20	<20	<20	<20	<20	93	154	152
As	10	888	2,200	83	65	260	<110	30	72
Se	7.4	32.3	42	9.1	16.2	9.3	3.5	4.2	6.3
Ag	2	4.6	5	<2	<2	<2	<2.6	<2	<3
Sb	16.5	72	39	9.4	5.3	3.7	1.4	1.2	11.8
Ba	620	540	46	98	36	88	260	520	42
Au	5.2	1.3	6.3	0.08	0.91	0.08	<0.01	<0.01	0.13
Hg	2.5	2.1	3.4	<1	<1.4	<1	2.9	<1.4	8.8
Te	10	<12	35	<5	6	6	<7	3	9
Rb (ppm)	<10	12	<10	14	<10	16	204	200	98
Sr	500	930	134	880	182	440	—	40	28
Y	<10	<10	<10	10	<10	<10	—	16	24
Zr	116	132	102	142	100	122	—	104	140
Nb	<10	<10	<10	<10	<10	<10	—	<10	<10
Rb/Sr	*<0.02*	*0.01*	*<0.75*	*0.02*	*<0.06*	*0.04*	—	*5.0*	*3.4*
La (ppm)	21.2	26.0	10.6	16.6	13.2	25.0	27.6	22.4	16.0
Ce	39.2	48.0	20.4	29.4	21.9	53.6	53.3	42.2	31.0
Nd	16.9	21.1	<40	10.5	10.6	22.0	26.3	21.8	16.2
Sm	4.68	2.25	1.37	1.95	1.69	4.80	4.04	3.73	3.10
Eu	0.63	1.26	0.81	0.17	0.31	1.28	0.82	0.98	0.63
Dy	0.94	0.96	0.75	0.90	0.89	1.78	3.09	3.08	3.55
Yb	0.80	0.84	0.92	0.93	0.82	0.93	1.91	1.49	2.01
Lu	0.11	0.18	<0.23	0.13	0.18	0.23	0.26	0.22	0.37

* Samples (abbreviations: Cinto ash-flow tuff = Caft, Lázaras ash-flow tuff = Laft): 87A230, Caft, pit No. 2, 290-m bench; 87A171a, rhyolite dome, pit No. 1, 290-bench; 87A285, Caft, pit No.1, 250-m bench; 87A169, rhyolite dome, pit No. 1, 290-bench; SRT60, breccia, DH-SP m. 60; SRT185, Caft, DH-SP m. 185; 87A209, rhyolite dome, W flank of Cerro Cinto; S2-20, Laft, DH-2 m. 20; S3-27, Laft, DH-3 m. 27.

¶ See cross section in Figure 3 for location of samples and distribution of alteration zones

§ Fe_2O_3 = total iron as Fe_2O_3

Major elements analyzed by wavelength-dispersive X-ray fluorescence (USGS, Denver; D.F. Siems and J.E. Taggart, analysts); Cu, Zn, Rb, Sr, Y, Zr, Nb, Ba analyzed by energy-dispersive XRF (USGS, Menlo Park); As, Se, Ag, Sb, Au, Hg, Te, and REE analyzed by instrumental thermal neutron activation (Phoenix Memorial Laboratory, University of Michigan, Ann Arbor)

Table 3. (Cont.) Chemical Composition of Altered Rocks Related to the Rodalquilar Gold Deposit, Spain

	Intermediate argillic zone (deep)			Sericitic zone			Propylitic zone			
Sample No.*	SRT378	87A83	87A44	SRT595	87A14	SRT830	S2-125	S2-322	S3-166	S3-418
Location¶	(10)	(11)	(12)	(13)	(14)	(15)	(16)	(17)	(18)	(19)
SiO_2 (wt %)	69.8	68.8	71.6	70.6	74.4	57.8	61.1	59.9	67.7	53.4
Al_2O_3	16.4	13.5	16.8	15.3	14.7	17.3	15.6	14.8	14.3	15.3
Fe_2O_3§	3.79	3.66	2.11	3.14	1.81	6.37	5.49	7.35	3.65	9.14
MgO	<0.10	0.75	<0.10	1.07	0.78	6.15	3.38	3.93	2.51	6.73
CaO	0.06	0.04	0.06	0.17	0.04	0.23	2.78	1.49	0.22	4.16
Na_2O	0.24	0.25	0.22	0.20	0.32	0.33	3.18	1.79	3.00	3.48
K_2O	0.48	3.75	0.66	4.35	4.06	3.52	3.62	3.85	4.83	0.34
TiO_2	0.47	0.47	0.46	0.46	0.29	0.68	0.54	0.52	0.33	0.61
P_2O_5	0.11	0.06	0.09	0.12	0.09	0.13	0.11	0.11	0.09	0.13
MnO	<0.02	<0.02	<0.02	<0.02	<0.02	<0.02	0.10	0.17	0.16	0.39
LOI 925°C	7.80	8.29	7.05	4.06	3.09	7.29	3.84	5.57	2.42	4.89
Total	99.27	99.59	99.17	99.49	99.6	99.82	99.74	99.48	99.21	98.57
Cu (ppm)	42	<20	<20	98	<20	26	<20	198	<20	<20
Zn	<20	42	32	<20	<20	42	255	310	750	540
As	132	75	37	45	<20	<30	<80	237	<100	<150
Se	9.5	5.5	5.2	7.0	3.3	15.4	3.6	3.0	3.1	<2.7
Ag	<3.2	<3.0	<2.3	2.3	<2.0	<3.3	<2.9	<3.2	<2.5	<3.7
Sb	3.0	2.9	3.6	1.3	0.5	2.9	3.3	3.6	4.5	5.4
Ba	38	—	—	210	110	196	265	490	570	44
Au	0.11	0.02	0.27	0.01	0.01	0.02	0.02	0.18	0.07	0.03
Hg	<2.0	2.2	10	<2.0	9.0	<2.0	<2	<2.0	6.8	6.6
Te	<5.7	<5	6	4.7	<5	<6	<5	9.2	7	<6
Rb (ppm)	<10	134	<10	182	152	138	132	152	200	14
Sr	144	—	—	<10	18	<10	138	98	54	132
Y	<10	—	—	26	24	20	34	24	34	28
Zr	120	—	—	125	120	75	104	105	102	82
Nb	<10	—	—	<10	<10	<10	<10	<10	<10	<10
Rb/Sr	*<0.07*	—	—	*>18*	*>8.4*	*>13*	*0.96*	*1.6*	*3.7*	*0.11*
La (ppm)	25.6	17.1	31.5	24.1	37.7	17.7	20.5	26.2	27.8	11.3
Ce	54.3	35.9	58.3	53.1	75.9	36.3	39.2	48.0	52.5	25.6
Nd	22.8	12.6	29.8	18.2	30.6	21.6	17.2	20.4	22.3	10.9
Sm	3.89	2.95	4.84	4.10	4.99	3.90	3.77	3.44	4.42	2.83
Eu	0.85	0.48	0.87	0.82	0.98	1.08	0.93	0.85	0.82	0.80
Dy	2.23	3.08	1.35	3.58	3.10	3.11	3.39	2.16	2.27	4.20
Yb	1.36	1.93	1.4	2.07	2.11	1.82	1.91	1.49	1.98	1.78
Lu	0.26	0.36	0.30	0.31	0.33	0.27	0.32	0.28	0.40	0.30

* Samples (abbreviations: Cinto ash-flow tuff = Caft, Lázaras ash-flow tuff = Laft): SRT378, Caft, DH-SP m. 378; 87A83, Laft, DH-1 m. 81; 87A44, Laft, DH-1 m. 276; SRT595, Caft, DH-SP m. 595; 87A14, Caft, DH-1 m. 480; SRT830, dacite tuff, DH-SP m. 830; S2-125, Laft, DH2 m.125; S2-322, Laft, DH-2 m. 322; S3-166, Caft, DH-3 m. 166; S3-418, precaldera andesite, DH-3 m. 418.

¶ See cross section in Figure 3 for location of samples and distribution of alteration zones

§ Fe_2O_3 = total iron as Fe_2O_3

Major elements analyzed by wavelength-dispersive X-ray fluorescence (USGS, Denver; D.F. Siems and J.E. Taggart, analysts); Cu, Zn, Rb, Sr, Y, Zr, Nb, Ba analyzed by energy-dispersive XRF (USGS, Menlo Park); As, Se, Ag, Sb, Au, Hg, Te, and REE analyzed by instrumental thermal neutron activation (Phoenix Memorial Laboratory, University of Michigan, Ann Arbor)

Table 4. Chemical Composition of Alunite from the Rodalquilar Deposit, Spain

	Stage 1 alunite (hypogene)			Stage 2 alunite (supergene)		
Sample No.≠	SRT133	87A237	88A06	87A97	87A373	87A380
Na_2O (wt %)◊	2.09	0.35	1.82	0.26	0.26	0.20
K_2O	7.74	7.59	8.05	10.00	10.13	8.30
MgO	0.00	0.01	0.01	0.02	0.04	0.07
BaO	0.03	0.03	0.13	0.03	0.06	0.13
CaO	0.01	0.04	0.22	0.00	0.02	0.14
SrO	0.03	0.08	0.10	0.09	0.13	0.12
Y_2O_3	0.00	0.00	0.00	0.00	0.00	0.00
La_2O_3	0.00	0.00	0.00	0.01	0.00	0.00
Ce_2O_3	0.00	0.00	0.01	0.00	0.02	0.01
Al_2O_3	36.94	25.80	34.53	34.30	34.20	28.24
Fe_2O_3	0.4	0.06	0.67	1.58	0.49	1.61
MnO	0.00	0.00	0.00	0.00	0.00	0.00
SO_3	38.80	27.00	36.10	35.65	35.76	29.00
P_2O_5	0.10	0.08	0.25	0.50	0.50	0.73
H_2O	13.20	9.50	12.40	13.40	13.60	11.40
TiO_2	0.01	0.30	0.05	0.02	0.01	0.02
Si_2O	nm	nm	nm	nm	nm	19.65
Total	99.35	70.84*	94.35	95.86	95.22	99.62
Difference§	—	29.16	5.65	4.14	4.78	—
	Number of atoms based on $(Al + Fe^{3+}) = 3$					
Na	0.28	0.07	0.26	0.04	0.04	0.03
K	0.68	0.95	0.75	0.92	0.95	0.95
Mg	0.00	0.00	0.00	0.00	0.00	0.01
Ca	0.00	0.00	0.01	0.00	0.00	0.01
Sr	0.00	0.00	0.01	0.00	0.00	0.01
Ba	0.00	0.00	0.00	0.00	0.00	0.00
Al	2.98	3.00	2.96	2.91	2.97	2.89†
Fe	0.02	0.00	0.04	0.09	0.03	0.11
S	1.99	2.00	1.97	1.93	1.98	1.95
P	0.01	0.01	0.02	0.03	0.03	0.06
H	6.03	6.24	6.02	6.44	6.69	6.63†
"excess" OH¥	—	0.24	—	0.44¶	0.69¶	0.63¶
Na/K	0.41	0.07	0.34	0.04	0.04	0.04
Other minerals in concentrate□	<10% zn < 3% qtz	25 ± 5% qtz	~ 5% qtz	< 3% qtz	None detected	< 3% qtz < 5% kao

Table 4. (Cont.) Chemical Composition of Alunite from the Rodalquilar Deposit, Spain

	Stage 1 alunite (hypogene)			Stage 2 alunite (supergene)		
Sample No.≠	SRT133	87A237	88A06	87A97	87A373	87A380
Cu (ppm)	56	<20	<20	126	—	255
Zn	<20	<20	<60	84	—	330
Rb	26	24	34	26	20	68
Sr	1,500	446	2,150	48	176	1,150
Y	<10	12	20	86	60	102
Zr	60	166	156	16	16	52
Nb	<10	<10	<10	<10	<10	<10
Ba	255	870	1,100	900	—	1,150
Au	0.15	0.04	<0.01	0.01	<0.01	0.02
La (ppm)	31.8	21.1	39.9	7.96	10.1	36.9
Ce	4.54	40.3	72.1	15.9	17.6	83.1
Nd	<4.9	13.3	35.3	18.8	11.4	73
Sm	0.652	2.58	2.66	3.13	5.09	14.5
Eu	0.692	0.773	0.517	0.797	1.58	3.51
Gd	<4.47	9.84	<4.4	<4.4	<5	8.27
Tb	<0.40	<0.44	<0.32	<0.44	0.84	1.78
Dy	<1	1.36	<0.9	1.98	<0.7	5.72
Yb	<0.14	0.994	0.338	<0.21	0.14	0.49
Lu	<0.03	0.193	0.063	<0.04	0.033	0.09

≠ Samples: SRT 133, DH-SP drill hole m. 133; 87A237, pit No. 2, 290-m bench; 88A06, pit No. 1, 290-m bench; 87A97, 150 m. east of 340 vein; 87A373, SW flank of Cerro Cinto; 87A380, NW flank of Cerro Cinto.

* Low total due to quartz; see "other minerals in concentrate".

§ Value shown = 100.00 – sum of measured oxides

† Excess Al above (Al + Fe):(S + P) = 3:2 assumed to be present in kaolinite. H corrected accordingly assuming kaolinite stoichiometry.

¥ Calculated on the basis of 6 (OH) per formula unit.

¶ Considering the results of X-ray analyses of samples, the "excess" water may be present as hydrated amorphous silica.

¤ Based on X-ray analysis: zn = zunyite, qtz = quartz, kao = kaolinite

◊ Analytical methods: Oxide components analyzed by induction coupled plasma mass spectrometry and atomic absorption techniques (Geological Survey of Japan, Tsukuba, M. Aoki, analyst); Cu, Zn, Rb, Sr, Y, Zr, Nb and Ba analyzed by energy-dispersive XRF (USGS, Menlo Park); Au and REE analyzed by instrumental thermal neutron activation (Phoenix Memorial Laboratory, University of Michigan, Ann Arbor)

Table 5. Chemical Composition of Chalcedonic-quartz Ore from the Rodalquilar Gold Deposit, Spain

	Black chalcedony					White chalcedony		
Sample No.*	87A171b	87A284a	87A240.1	87A316	87A138	87A171c	87A284b	87A137
SiO_2 (wt %)	86.2	86.8	—	—	—	88.4	88.1	—
Al_2O_3	1.66	0.97	—	—	—	2.42	2.23	—
Fe_2O_3§	4.51	5.07	—	—	—	2.68	2.42	—
MgO	<0.10	<0.10	—	—	—	<0.10	<0.10	—
CaO	0.1	0.05	—	—	—	0.03	0.06	—
Na_2O	0.17	0.17	—	—	—	0.24	0.28	—
K_2O	0.24	0.31	—	—	—	0.47	0.45	—
TiO_2	0.25	0.40	—	—	—	0.23	0.50	—
P_2O_5	0.37	0.14	—	—	—	0.12	0.26	—
MnO	<0.02	<0.02	—	—	—	<0.02	<0.02	—
LOI 925°C	3.94	4.15	—	—	—	3.85	4.26	—
Total	97.56	98.18	—	—	—	98.56	98.68	—
Cu (ppm)	910	2,600	5,500	5,000	420	38	34	370
Zn	<20	<20	<20	<20	<20	<20	<20	<20
As	11,800	130	355	466	3,240	2,300	740	13,800
Se	92	94	135	36	64	42	25	53
Ag	18	6	18	46	9	5	<2	<2
Sn	900	<300	340	<220	180	1,100	<250	310
Sb	2,380	230	108	41	406	865	128	506
Ba	98	60	168	38	52	134	60	210
Au	33.5	13.3	240	6.6	44.3	5.2	5.1	1.0
Hg	42	11	57	20	15	4.0	5.3	8.2
Te	75	25	108	14	406	52	18	506
Rb (ppm)	90	22	16	<10	12	22	22	10
Sr	2,700	880	770	<10	475	660	880	920
Y	22	<10	<10	<10	<10	<10	<10	<10
Zr	130	110	54	38	72	74	110	72
Nb	<10	<10	<10	<10	<10	<10	<10	<10
Rb/Sr	*0.033*	*0.025*	*0.021*		*0.025*	*0.033*	*0.025*	*0.011*
La (ppm)	44.4	18.0	8.0	14.7	20.9	15.2	24.8	13.4
Ce	81.3	34.7	15.7	27.0	39.3	30.5	44.0	22.9
Nd	<78	17.0	9.8	20.0	<51	<46	18.7	<63
Sm	4.03	2.08	1.12	2.92	2.40	1.21	2.78	1.59
Eu	2.98	1.02	1.49	2.84	0.98	0.70	0.86	0.66
Dy	<0.9	<0.7	<0.5	<0.6	0.34	<0.7	0.83	<0.8
Yb	<2.5	0.43	<0.2	0.3	<1.3	<1.3	0.65	<1.8
Lu	<0.5	0.17	0.1	0.05	<0.3	<0.3	0.12	<0.4

* Samples: 87A171b, pit No. 1 , 270-m bench; 87A284a, pit No.1, 250-m bench; 87A240.1, pit No.2, 230-m bench, 87A316, Maria Josefa vein 20 m below surface (elev. = 250 m); 87A138, pit No.1, 250-m bench; 87A171c, pit No.1, 290-m bench; 87A284b, pit No.1, 250-m bench; 87A137, pit No.1, 250-m bench.

§ Fe_2O_3 = total iron as Fe_2O_3

Major elements analyzed by wavelength-dispersive X-ray fluorescence (USGS, Denver; D.F. Siems and J.E. Taggart, analysts); Cu, Zn, Rb, Sr, Y, Zr, Nb, Ba analyzed by energy-dispersive XRF (USGS, Menlo Park); As, Se, Ag, Sn, Sb, Au, Hg, Te, and REE analyzed by instrumental thermal neutron activation (Phoenix Memorial Laboratory, University of Michigan, Ann Arbor)

Table 6. Summary of Freezing and Homogenization Results for Fluid Inclusions from the Rodalquilar deposit

Host mineral	Sample no. (drill hole, depth)	Inclusion type[1]	Freezing			Homogenization		
			T_m range (°C)	Mean (°C)	n	T_h range (°C)	Mean (°C)	n
Quartz phenocrysts	S2-124 (DH-2, 124 m)	I	(-1.4) - (-6.2)	-2.9	15	210 - 298	261	38
	S2-322 (DH-2, 322 m)	I	(-2.7) - (-9.2)	-6.6	39	181 - 385	287	39
	S3-68 (DH-3, 68 m)	I	(-2.2) - (-5.2)	-3.1	12	239 - 257	251	12
	S3-350 (DH-3, 350 m)	I	(-1.5) - (-5.4)	-3.4	37	242 - 298	266	41
	87A10 (DH-1, 440 m)	III	(-14.3) - (-31.0)	-25.2	23	365 - 407	395	23
		III	260[2] - 295[2]	285	4	385 - 425	404	4
Hydrothermal quartz	87A14 (DH-1, 480 m)	I	(-1.5) - (-10.2)	-5.9	59	216 - 425	348	59
		II	(-1.7) - (-4.7)	-2.4	5	315 - 450	366	14
		III	323[2] - 387[2]	345	8	>500		8

[1] I = liquid-rich, homogenization to liquid; II = vapor-rich, homogenization to vapor; III = multiphase with up to four daughter minerals, homogenization to liquid and vapor

[2] Halite melting temperature

Table 7. Fluid Inclusion Data for Sample 87A14 (DH-1 m 480m)

Tm (°C)	wt% NaCl eq.*	Th^ (°C)	Comments	Tm (°C)	wt% NaCl eq.*	Th^ (°C)	Comments
	~40%	>500	Tm(h) = 325°C•	-8.5	12.2	404	
	~40%	>500	Tm(h) = 323°C•	-4.5	7.1	392	
	~45%	>500	Tm(h) = 387°C•	-3.5	5.6	254	
	~42%	>500	Tm(h) = 361°C•	-4.5	7.1	396	
			Tm (a) = <135°C "	-5.1	7.9	420	
	~42%	>500	Tm(h) = 352°C•	-7.5	11.0	406	
			Tm (a) = <135°C "	-7.3	10.7	400	
	~40%	>500	Tm(h) = 325°C•	-7.1	10.5	414	
			Tm (a) = 138°C "	-6.3	9.5	425	
	~42%	>500	Tm(h) = 365°C•	-7.5	11.0	423	
	~40%	>500	Tm(h) = 325°C•	-7.6	11.1	411	
-1.7	3.0	315	Th(v)	-6.3	9.5	410	
-1.8	3.1	368	Th(v)	-7.7	11.2	414	
-1.9	3.3	452	Th(v)	-7.9	11.5	398	
-2.1	3.6	425	Th(v)	-8.3	12.0	434	
-4.7	7.3	440	Th(v)	-6.1	9.2	411	
		338	Th(v), no ice formed	-7.1	10.5	425	
		340	Th(v), no ice formed	-6.4	9.6	422	
		335	Th(v), no ice formed	-4.7	7.3	405	
		380	Th(v), no ice formed	-2.9	4.8	237	
		336	Th(v), no ice formed	-2.8	4.6	247	
		345	Th(v), no ice formed	-2.8	4.6	230	
		352	Th(v), no ice formed	-2.7	4.5	216	
		344	Th(v), no ice formed	-2.5	4.2	232	
		348	Th(v), no ice formed	-7.4	10.9	352	
-9.1	12.9	407		-3.5	5.6	289	
-7.5	11.0	385		-9.2	13.0	368	
-7.6	11.1	418		-10.2	14.1	390	
-6.6	9.9	395		-9.1	12.9	382	
-6.4	9.6	398		-1.6	2.8	222	
-6.8	10.1	397		-1.5	2.7	220	
-8.6	12.3	376		-2	3.4	239	
-8.8	12.6	361		-2.1	3.6	250	
-8.4	12.1	383		-2.2	3.7	246	
-8.8	12.6	368		-2.3	3.9	279	
-8.9	12.7	354		-2.1	3.6	277	
-6.8	10.1	381		-2.2	3.7	282	
-9	12.8	370		-3.2	5.2	370	
-9.3	13.1	388		-2.2	3.7	278	
-8.6	12.3	376		-3	4.9	248	
-7	10.4	395		-4.7	7.3	243	
-9.7	13.6	380		-3.4	5.5	255	

* Calculated using Hall et al. (1988) equation for NaCl/(NaCl + KCl) = 1.0, except where noted (see •)

• Tm(h) = Temperature of melting of halite. Salinity calculated based on NaCl saturation curve in Holland and Mailinin (1979). This is a minimum value since KCl is present in solution

" Tm(a) = Temperature of melting of an unknown anisotropic phase

^ Temperature of homogenization to liquid except where Th(v) = temperature of homogenization to vapor

Table 8. Microthermometric data of secondary fluid inclusions in quartz phenocrysts: sample S2-124 (DH-2 drill hole, 124 m depth)

Tm (°C)	wt% NaCl eq.	Th (°C)
-4.0	6.4	275
-2.6	4.3	279
-2.2	3.7	265
-1.5	2.7	254
-1.4	2.5	276
-1.7	3.0	259
-1.9	3.3	298
-2.5	4.2	260
-6.2	9.3	230
-5.2	8.0	230
-4.4	6.9	210
-3.1	5.1	235
-3.2	5.2	245
-1.7	3.0	259
-1.9	3.3	298
		272
		241
		238
		237
		285
		235
		225
		270
		280
		261
		294
		258
		287
		270
		272
		261
		258
		257
		292
		249
		246
		277
		288

All fluid inclusions are liquid-rich (type I) with homogenization to liquid

Table 9. Microthermometric data of secondary fluid inclusions in quartz phenocrysts: sample S2-322 (DH-2 drill hole, 322 m depth)

Tm (°C)	wt% NaCl eq.	Th (°C)
-2.7	4.5	181
-3.8	6.1	210
-3.6	5.8	221
-3.7	5.9	230
-3.9	6.2	232
-3.9	6.2	230
-7.0	10.4	358
-6.6	9.9	359
-6.5	9.7	359
-6.8	10.1	359
-6.8	10.1	360
-7.4	10.9	284
-8.0	11.6	278
-8.3	12.0	277
-7.8	11.4	282
-8.5	12.2	272
-8.7	12.4	269
-8.4	12.1	266
-2.8	4.6	214
-3.0	4.9	212
-8.9	12.7	275
-6.1	9.2	276
-9.1	12.9	272
-8.0	11.6	381
-8.6	12.3	385
-7.8	11.4	384
-3.9	6.2	279
-4.1	6.5	278
-3.9	6.2	277
-3.9	6.2	278
-3.9	6.2	275
-8.6	12.3	266
-8.0	11.6	268
-9.1	12.9	270
-9.0	12.8	350
-8.9	12.7	269
-8.8	12.6	272
-9.1	12.9	349
-9.2	13.0	348

All fluid inclusions are liquid-rich (type I) with homogenization to liquid

Table 10. Microthermometric data of secondary fluid inclusions in quartz phenocrysts: sample S3-68 (DH-3 drill hole, 68 m depth)

Tm (°C)	wt% NaCl eq.	Th (°C)
-2.2	3.7	253
-2.2	3.7	250
-2.2	3.7	252
-2.2	3.7	257
-4.6	7.2	251
-4.7	7.3	256
-4.7	7.3	247
-2.4	4.0	249
-5.2	8.0	239
-2.3	3.9	256
-2.3	3.9	253
-2.3	3.9	248

All fluid inclusions are liquid-rich (type I) with homogenization to liquid

Table 11. Microthermometric data of secondary fluid inclusions in quartz phenocrysts: sample S3-350 (DH-3 drill hole, 350 m depth)

Tm (°C)	wt% NaCl eq.	Th (°C)	Comments
-3.2	5.2	288	
-3.2	5.2	276	
-3	4.9	278	
-3.1	5.1	282	
-3	4.9	281	
-3.5	5.6	251	
-1.5	2.7	262	
-2	3.4	252	
-2.0	3.4	260	
-3.5	5.6	255	
-1.5	2.7	251	
-3.3	5.4	258	
-2.2	3.7	249	
-3.0	4.9	198	
-3.0	4.9	298	
-3.1	5.1	277	
-2.4	4.0	237	
-3.0	4.9	283	
-3.0	4.9	291	
-3.8	6.1	258	
-3.9	6.2	258	
-3.8	6.1	262	
-3.9	6.2	261	
-3.4	5.5	268	
-3.3	5.4	261	
-4.9	7.6	267	
-4.9	7.6	262	
-4.8	7.5	264	
-4.9	7.6	262	
-3.6	5.8	268	
-3.2	5.2	271	
-4.9	7.6	267	
-5.4	8.3	272	
-4.9	7.6	272	
-5.4	8.3	269	
-3.2	5.2	242	
-2.9	4.8	274	
		260	
		263	
		264	
		263	

All fluid inclusions are liquid-rich (type I) with homogenization to liquid

Table 12. Microthermometric data of secondary fluid inclusions in quartz phenocrysts: sample 87A10 (DH-1 drill hole, 440 m depth)

Tm (°C)	wt% NaCl eq.	Th (°C)	Comments
-24.7	24.5	365	
-24.8	24.5	375	
-24.4	24.4	375	
-25.0	24.6	375	
-18.7	21.5	385	
-28.0	25.3	385	
-24.2	24.3	395	
-24.8	24.5	395	
-29.5	25.5	395	
-31.0	25.6	396	
-29.4	25.5	398	
-14.5	18.4	400	
-23.2	23.9	400	
-23.4	24.0	402	
-30.0	25.6	402	
-29.7	25.5	403	
-14.3	18.2	405	
-32.0	25.6	405	
-24.1	24.3	405	
-24.2	24.3	405	
-26.1	24.9	405	
-24.6	24.5	406	
-29.4	25.5	407	
	37.0	385	Tm halite 295
	37.0	400	Tm halite 290
	34.0	406	Tm halite 260
	37.0	425	Tm halite 294

Table 13. Summary of Sulfur, Hydrogen, and Oxygen Isotope Ratios for Samples from the Rodalquilar Deposit

	$\delta^{34}S$				δD				$\delta^{18}O_{silicate}$ or $\delta^{18}O_{OH\ sulfate}$				$\delta^{18}O_{SO_4}$			
Sample analyzed	Range (‰)	Mean (‰)	σ (‰)	n	Range (‰)	Mean (‰)	σ (‰)	n	Range (‰)	Mean (‰)	σ (‰)	n	Range (‰)	Mean (‰)	σ (‰)	n
Alunite stg. 1	22.3 – 31.0	28.5	2.6	10	(-15) – (-26)	-21	4.1	9	11.9 – 13.8	12.7	1.0	3	10.8 – 18.6	15.6	2.7	10
Alunite stg. 2	5.6 – 10.2	7.4	1.2	21	(-18) – (-48)	-26	7	17	10.5 – 16.3	12.5	2.1	6	4.1 – 10.4	7.1	1.6	22
Barite	28.9			1									12.6			1
Igneous biotite					-90			1	9.6			1				
Black chalcedony	2.0 – 6.2	4.6	1.2	15					12.4 – 14.7	13.9	0.8	6				
Galena	0.9 – 3.3	2.6	1.0	5												
Hydrothermal qtz									11.9 – 14.6	13.2	1.0	6				
Illite					(-27) – (-46)	-36	8.3	4	8.8 – 12.7	10.0	1.4	6				
Jarosite	5.3 – 10.3	8.6	2.9	3	(-58) – (-97)	-83	17	4	10.2			1	6.0			1
Kaolinite stg. 1					(-36) – (-39)	-38		2	14.9 – 15.6	15.3		2				
Kaolinite stg. 2					(-41) – (-72)	-56	14	5	16.0 – 21.2	18.5	2.3	4				
Meteoric water					(-31) – (-42)	-36	5	8								
Pyrite	0.3 – 8.0	5.0	1.5	34												
Igneous quartz									11.2			1				
Silicified pyroclastic unit									16.5 – 19.6	18.5	1.8	3				
Sphalerite	4.0 – 6.1	5.1	0.8	5												
Volcanic rock	0.6 – 7.3	4.5		4												
Vuggy silica									12.6			1				
White chalcedony									12.8 – 14.9	13.9	1.5	2				

Table 14. $\delta^{34}S$ Values of Sulfides and Whole-Rock Samples from the Rodalquilar Deposit

Sample	Location	Mineral[1]	$\delta^{34}S$ (‰)	Remarks
86A165-A	host-rock 340 vein	py	6.8	>500 μm separate
86A165-B	host-rock 340 vein	py	6.9	<500 μm separate
86A177	Pit 3, 240-m bench	py	5.9	
86A173-A	Pit 2, Raquel mine	py	4.1	>500 μm separate
86A173-B	Pit 2, Raquel mine	py	4.1	<500 μm separate
C-III	Pit 3, 210-m bench	py	5.1	
87A10	DH-1 m. 441	py	4.4	
87A14	DH-1 m. 480	py	3.7	
87A18	DH-1 m. 409	py	4.4	
87A21	DH-1 m. 367	py	3.8	
87A36f	DH-1 m. 292	py	8.0	
87A41	Triunfo vein	py	5.0	
87A44	DH-1 m. 285	py	0.3	
87A47	DH-1 m. 267	py	4.7	
87A48	DH-1 m. 262	py	4.9	
87A49	DH-1 m. 290	py	6.1	
87A50-I	DH-1 m. 228	py	3.7	Core of pyrite crystal
87A50-E	DH-1 m. 228	py	2.4	Rim of pyrite crystal
87A67	DH-1 m. 180	py	4.1	
87A83	DH-1 m. 81	py	4.2	
87A85	340 vein	py	6.1	
87A110	DH-SP m. 128	py	6.5	T (°C) py-al[2] = 280
87A111	DH-SP m. 130	py	5.7	T (°C) py-al[2] = 250
87A113	DH-SP m. 247	py	4.3	
87A120	DH-SP m. 191	py	4.9	T (°C) py-al[2] = 330
87A121	DH-SP m. 429	py	7.0	
87A123	DH-SP m. 596	py	5.8	
87A124	DH-SP m. 695	py	5.9	
87A125	DH-SP m. 760	py	4.7	
87A150	Pit 1, 270-m bench	py	5.9	T (°C) py-al[2] = 220
87A165	Pit 1, 270-m bench	py	3.8	
87A336	Mi Lucía mine	py	6.2	
87A367	340 vein	py	6.5	
S2-322	DH-2 m. 322	py	5.6	

Table 14. (Cont.) $\delta^{34}S$ values of sulfides and whole-rock samples from the Rodalquilar Deposit

Sample	Location	Mineral	$\delta^{34}S$ (‰)	Remarks
Other sulfides				
87A58	Consulta	ga	3.0	
87A67	DH-1 m. 180	sp	4.7	
87A41	Triunfo	sp	5.4	T (°C) sp-ga[3] = 130
87A41	Triunfo	ga	0.9	
Trfo-1	Triunfo vein	sp	4.0	T (°C) sp-ga[3] = 500
Trfo-1	Triunfo vein	ga	2.8	
87A88	Las Niñas vein	sp	6.1	T (°C) sp-ga[3] = 250
87A88	Las Niñas vein	ga	3.3	
87A90	Las Niñas vein	sp	5.4	T (°C) sp-ga[3] = 250
87A90	Las Niñas vein	ga	2.8	
Sulfides in black chalcedony[4]				
86A195-1	Pit 3	py (bc)	6.2	
86A195-2	Pit 3	py (bc)	2.6	
87A93	340 vein	py (bc)	5.3	
87A102	DH-SP m39	py (bc)	5.8	
87A116	Pit No. 2, 250-m bench	py (bc)	5.5	
87A126	Pit No. 1, 230-m bench	py (bc)	4.7	
87A138	Pit No. 1, 250-m bench	py (bc)	5.9	
87A184	María Josefa mine	py (bc)	4.9	
87A240	Pit 2, 230-m bench	py (bc)	3.0	
87A282	Pit 2, 230-m bench	py (bc)	3.7	
87A284	Pit 1, 250-m bench	py (bc)	4.1	
87A314	María Josefa mine	py (bc)	4.9	
87A316-1	María Josefa mine	py (bc)	3.2	
87A316-2	María Josefa mine	py (bc)	2.0	
87A323	María Josefa mine	py (bc)	6.0	
Unaltered volcanic rock[5]				
88BA50	Cinto ash-flow tuff	wr	5.0	
87ALAZ	Lázaras ash-flow tuff	wr	4.9	
86A50	Hornblende andesite flow	wr	7.3	
87A343	Younger pyroxene andesite	wr	0.6	

1 Abbreviations: py = pyrite, sp = sphalerite, ga = galena, py (bc)= disseminated sulfides (chiefly pyrite) in black chalcedony, wr = whole rock

2 Calculated from $\delta^{34}S_{alunite}$ and $\delta^{34}S_{pyrite}$ using equations for fractionation FeS_2-H_2S (Ohmoto and Rye, 1979) and SO_4-H_2S (Ohmoto and Lasaga, 1982)

3 Calculated from $\Delta = \delta^{34}S_{sp} - \delta^{34}S_{ga}$ using equation of Ohmoto and Rye (1979)

4 Sulfur in sample extracted as H_2S and converted to Ag_2S prior to $^{34}S/^{32}S$ analysis

5 Sulfur extracted using a modified Kiba technique (Sasaki et al., 1979; Ueda and Sakai, 1983)

Table 15. $\delta^{34}S$ Values of Alunites, Jarosites and Barites from the Rodalquilar Deposit

Sample	Location	Mineral[1]	δD (‰)	$\delta^{18}O_{SO4}$ (‰)	$\delta^{18}O_{OH}$ (‰)	$\delta^{34}S$ (‰)	Remarks
86SC14A	Cinto	al 1	-16	16.5		30.0	
86SC14B	Cinto	al 1		17.9		28.7	
87A110	DH-SP m.128	al 1	-26	10.8		26.5	$T_{(al\text{-}py)}^2$ = 280°C
87A111	DH-SP m. 130	al 1	-23	13.9	11.9	28.8	$T_{(SO4\text{-}OH)}^3$ = 620°C, $T_{(al\text{-}py)}^2$ = 250°C K/Ar age= 10.4 ± 0.6 Ma
87A120	DH-SP m. 191	al 1	-19	11.7		22.3	$T_{(al\text{-}py)}^2$ = 330°C
87A150	Pit 1, 270-m bench	al 1	-20	16.7	13.8	31.0	$T_{(SO4\text{-}OH)}^3$ = 330°C, $T_{(al\text{-}py)}^2$= 220°C K/Ar age= 10.1 ± 0.6 Ma
87A187	Pit 1, 270-m bench	al 1	-26	17.3		30.6	
87A225	Cinto, 230-m bench	al 1	-15	17.7		30.2	
87A237	Pit 2, 270-m bench	al 1	-24	18.6		29.2	
88A06	Pit 1, 210-m bench	al 1	-19	15.2	12.3	27.7	$T_{(SO4\text{-}OH)}^3$ = 380°C
87A223	Vein at Cerro de la Cruz	ba		12.6		28.9	
1985RR1	Cinto	al 2		5.7		8.4	
1985RR2	Cinto	al 2		10.4		7.2	
1985RR3	Cinto	al 2		4.1		6.8	
86SC12A	Cinto	al 2	-48	7.4		8.6	
86SC12B	Cinto	al 2		4.9		7.5	
86A31A	Pit 3, 250-m bench	al 2	-25	6.7		8.9	
86A32	Pit 3, 250-m bench	al 2	-24	4.2	13.5	5.6	K/Ar age= 3.0 ± 0.2 Ma
87A21	DH-1 m. 367	al 2	-28	7.6	16.3	8.1	
87A36f	DH-1 m. 290	al 2	-18	9.2		8.4	
87A40	Hortichuelas dome	al 2		4.8			
87A67	DH-1 m. 180	al 2	-23	9.2		8.5	$^{40}Ar/^{39}Ar$ age = 2.95±0.07 Ma
87A82	DH-1 m. 98	al 2	-24	7.4		6.2	
87A83	DH-1 m. 81	al 2	-28	7.0		7.0	
87A84	DH-1 m. 78	al 2	-25	7.6		6.1	
87A97	150 m east of 340 Vein	al 2	-20	7.1	11.3	8.2	K/Ar age= 3.8 ± 0.1 Ma
87A111.2	DH-1 m. 111	al 2	-25	8.3	12.1	7.1	
87A298	North flank of Cerro Cinto	al 2	-20	7.1		6.7	
87A363	S flank of C. Cinto	al 2	-37	7.7		6.0	
87A373	SW flank of C. Cinto	al 2	-26	6.7	11.3	6.7	K/Ar age= 3.1 ± 0.1 Ma
87A380	NW flank of C. Cinto	al 2	-35	8.2		7.8	K/Ar age= 3.5 ± 0.2 Ma
88A20	Road to Rodalquilar	al 2	-21	8.2	10.5	10.2	
S1-m47	DH-1 m.47	al 2	-23	6.2		6.1	
87A84	DH-1 m. 78	ja	-87			5.3	
S1m45	DH-1 m. 45	ja	-58				
87A237	Pit 2, 270-m bench	ja	-97	10.2	7.0	10.3	
87A279	Pit 2, 210-m bench	ja	-89			10.3	

[1] al 1 = Alunite Stage 1, al 2 =Stage 2 alunite, ba = barite, ja = jarosite

[2] Calculated from $\delta^{34}S_{alunite}$ and $\delta^{34}S_{pyrite}$ using equations for fractionation FeS_2-H_2S (Ohmoto and Rye, 1979) and SO_4-H_2S (Ohmoto and Lasaga, 1982)

[3] Calculated from $\Delta^{18}S_{SO_4\text{-}OH}$ values using experimentally derived equation of Stoffregen et al. (1994)

Table 16. Stable Isotope Data of Silicates and Meteoric Waters Related to the Rodalquilar Deposit

Sample No.	Mineral[1]	Location	δD (‰)	$\delta^{18}O$ (‰)	Remarks[2]
87A254***	kaol 1	Pit 2, 270-m bench	-39	15.6	microdrilling ~25% al, ja, q
87A165***	kaol 1	Pit 1, 270-m bench	-36	14.9	microdrilling <10% al, q
88A51	kaol 2	Cinto-Rodalquilar road, near San Diego mine	-72	17.2	2-0.25 μm separate ~30% il
88BA40	kaol 2	Kaolinite pits Lázaras ravine	-66	19.5	<0.25 μm separate <10% q, il
88A43	kaol 2	Kaolinite pits Lázaras ravine	-61	16.0	<0.25 μm separate ~20% il
88A61	kaol 2	Alunite-kaolinite pits Los Tollos	-41	21.2	<0.25 μm separate ~5% pi
88A63b	kaol 2	Alunite-kaolinite pits Los Tollos	-42		<0.25 μm separate <5% al
87A14	hq	DH-1 m 480		14.3	$T_{sericite\text{-}quartz}$[3] = 230°C
87A88	hq	Las Niñas vein		12.7	T[4] = 250°C
87A90	hq	Las Niñas vein		14.6	T[4] = 250°C
Trfo-1	hq	Triunfo		13.0	
87A49	hq	DH-1 m.290		12.9	
87A36f	hq	DH-1 m.292		11.9	
87A152	wch	Pit 1, 250-m bench		14.9	
87A94	wch	340 vein		12.8	
87A102	bch	DH-SP, m. 39		12.4	
87A116	bch	Cinto		14.2	
87A138	bch	Pit 1 270-m bench		14.4	
87A195-1	bch	Pit 2, 270-m bench		13.7	
87A240-2	bch	Pit 2, 230-m bench		14.7	
87A284	bch	Pit 1, 250-m bench		13.8	
87A21	il	DH-SP m. 367	-27	9.8	
87A14	il	DH-1 m. 480	-46	9.6	
87A123	il	DH-SP m. 596	-40	9.7	
87A18	il	DH-1 m.409	-33	12.7	
87A10	il	DH-1 m. 440		9.3	
87A125	il	DH-SP m.760		8.8	
87A344	bio	Cinto ash-flow tuff	-94	9.6	
87A344	iq	Cinto ash-flow tuff		11.2	
87A194	ss	Pit 2, 270-m bench		12.6	
88A26	sr			16.5	
88A29	sr			19.5	
88A42	sr			19.6	
A-86-1	mw	Consulta mine, Rodalquilar		-42	Collected Jul. 1986
A-88-5	mw	Well, Horticuelas		-35	Collected Dec. 1988
A-88-6	mw	Los Almendros aljibe		-32	Collected Dec. 1988
A-87-1	mw	San Pedro, spring water		-32	Collected Aug. 1987
A-87-1	mw	Férnan Perez, aljibe		-34	Collected Aug. 1987
A-87-3	mw	Los Cortijos Grandes aljibe		-31	Collected Aug. 1987
A-88-1	mw	Well No. 5, Sector 1, Níjar		-47	Collected Aug. 1988
A-88-2	mw	Well No. 8, Sector 1, Níjar		-41	Collected Aug. 1988
A-88-3	mw	Well No. 3, Sector 2, Níjar		-42	Collected Aug. 1988

[1] kaol 1 = kaolinite stage 1, kaol 2 = kaolinite stage 2, il =illite/ sericite, hq = hydrothermal quartz, ss = sugary silica, bch = black chalcedony, wch = white chalcedony, sr = silicified pyroclastic unit, mw = well water, bio = igneous biotite, iq = igneous quartz

[2] Abbreviations: al =alunite, ja = jarosite, q = quartz, pi = pyrophillite, il = illite and illite-montmorillonite

[3] Calculated from $\Delta^{18}O_{illite\text{-}quartz}$ values using equation of Eslinger et al. (1979)

[4] Temperature for sphalerite-galena pair of same specimen (see Table 14)

Table 17. Summary of Isotope Fractionation Equations Used in this Study

Element	Fractionation	Temperature range (°C)	Reference
Oxygen	$10^3 ln\alpha_{alun(OH)\text{-}H_2O} = 2.28 \times 10^6 T^{-2} - 3.90$	250 - 450	Stoffregen et al. (1994)
do	$10^3 ln\alpha_{alun(SO_4)\text{-}H_2O} = 3.09 \times 10^6 T^{-2} - 2.94$	250 - 450	Stoffregen et al. (1994)
do	$10^3 ln\alpha_{alun(SO_4\text{-}OH)} = 0.8 \times 10^6 T^{-2} + 1.0$	250 - 450	Stoffregen et al. (1994)
do	$10^3 ln\alpha_{kao\text{-}H_2O} = 2.50 \times 10^6 T^{-2} - 2.87$		Savin and Lee (1988)
do	$10^3 ln\alpha_{qtz\text{-}H_2O} = 3.34 \times 10^6 T^{-2} - 3.34$	150 - 500	Matsuhisa et al. (1979)
do	$10^3 ln\alpha_{amorph.\ sil\text{-}H_2O} = 3.52 \times 10^6 T^{-2} - 4.35$	30 - 100	Kita et al. (1985)
do	$10^3 ln\alpha_{ill\text{-}H_2O} = 2.43 \times 10^6 T^{-2} - 4.80$	160 - 270	Eslinger and Savin (1973)[1]
Sulfur	$10^3 ln\alpha_{SO_4\text{-}H_2S} = 6.46 \times 10^6 T^{-2} + 0.56$		Ohmoto and Lasaga (1982)
do	$10^3 ln\alpha_{FeS_2\text{-}H_2S} = 0.4 \times 10^6 T^{-2}$	200 - 700	Ohmoto and Rye (1979)
do	$10^3 ln\alpha_{SO_4\text{-}py} = 4.86 \times 10^6 T^{-2} + 6.0$		Ohmoto and Rye (1979)

Hydrogen	Temperature (°C)							Reference
	400	350	300	250	200	150	25	
Kaolinite-H_2O			-13	-14	-17	-19	-30	Marumo et al. (1980)
Alunite-H_2O	-18	-12	-10	-6	-6	-6	4[1]	Stoffregen et al. (1994)

[1] Bird et al. (1989)

Abbreviations: alun = alunite, kao = kaolinite, qtz = quartz, amorph. sil. = amorphous silica, ill = illite, py = pyrite

Table 18. Strontium Isotope ratios for Rodalquilar Whole Rocks and Mineral Separates

Rock group/ Sample no.	Rock type	Rb (ppm)	Sr (ppm)	$^{87}Sr/^{86}Sr$ (meas.)[1]	$^{87}Sr/^{86}Sr$ (correct.)[2]
Metamorphic basement rocks					
87A352	mica-schist (Pz)	138	98	0.72586	0.72528
87A353	mica-schist (Pz)	128	166	0.72476	0.72444
87A355	black schist (Pz)	155	405	0.71512	0.71496
87A358	mica-schist (Pz)	156	108	0.72960	0.72900
87A361	quartzite (TrP)	<10	114	0.71331	–
89FT1	limestone (JTr)	<10	40	0.70805	–
89FT2	dolostone (JTr)	<10	66	0.70896	–
89FT3	dolostone (JTr)	<10	60	0.71041	–
Miocene calc-alkalic volcanic rocks of the Cabo de Gata volcanic field					
86A189	precald andesite	235	200	0.71191	0.71123
88BA17	precald andesite	188	210	0.71158	0.71109
88BA50	Cinto	124	172	0.71351	0.71315
87A344	Cinto	196	170	0.71392	0.71335
86A43	Cinto	555	62	0.71801	0.71359
87A371	ring dome	146	160	0.71455	0.71410
87A372	ring dome	134	146	0.71444	0.71399
LAZ	Laz	116	70	0.71394	0.71312
HPOR	hbl andesite	52	130	0.71155	0.71139
86A50	hbl andesite	85	172	0.71209	0.71132
LLOB	pyx andesite	62	225	0.71318	0.71309
87A343	pyx andesite	18	336	0.71014	0.71012
Altered volcanic rocks and alunite					
SRM160	Cinto, adv. arg.	<10	352	0.71367	0.71367
87A14	Cinto, ser.	152	18	0.71452	0.71372
87A180	Cinto, adv. arg.	10	710	0.71350	0.71349
87A178	Cinto, adv. arg	10	6,700	0.71310	0.71310
87A169	Cinto, adv. arg.	14	882	0.71104	0.71103
87A240-1	Black chalc.	16	770	0.71461	0.71460
87A138	Black chalc.	12	475	0.71445	0.71444
87A284A	Black chalc.	22	880	0.71436	0.71435
SRTM378	Cinto, ser.- arg.	<10	144	0.71340	0.71338
SRTM185	Cinto, adv. arg.	16	140	0.71392	0.71390
SRTM60	Cinto, adv. arg.	<10	182	0.71413	0.71413
S2M322	Laz, prop.	152	98	0.71427	0.71364
S2M125	Laz, prop.	132	138	0.71394	0.71355
S2M20	Laz, arg.	200	40	0.71513	0.71310
S3M418	Andesite, prop.	14	132	0.71342	0.71338
S3M166	Laz, prop.	200	54	0.71525	0.71376
S3M27	Laz, adv. arg.	96	28	0.71501	0.71353
88A6	Alunite stg. 1	34	2,150	0.71357	0.71356
87A237	Alunite stg. 1	24	446	0.71326	0.71324
SRTM133	Alunite stg. 1	26	1,500	0.71245	0.71244
87A223	Barite	100	7,800	0.71409	0.71408
88A20	Alunite stg. 2	24	420	0.71040	0.71039
86A32	Alunite stg. 2	20	156	0.71139	0.71137
87A373	Alunite stg. 2	20	176	0.71213	0.71211
87A380	Alunite stg. 2	68	1,150	0.71185	0.71184
87A363	Alunite stg. 2	52	265	0.71103	0.71100
87A97	Alunite stg. 2	26	48	0.71419	0.71411
87A237JA	Jarosite	26	370	0.71168	0.71167

Abbreviations: Pz = Paleozoic, TrP = Permian and Early Triassic, J-Tr = Middle to Late Triassic, precald = precaldera, Cinto = Cinto ash-flow tuff, Laz = Lázaras ash-flow tuff, hbl = hornblende, pyx = pyroxene, ser. = sericitic alteration, arg. = argillic alteration, adv. arg. = advanced argillic alteration, prop. = propylitic alteration, black chalc. = black chalcedony

[1] Present-day measured values. Analytical uncertainty on isotopic compositions is < 0.1 percent

[2] Isotope ratios corrected for in situ decay (t = 10 Ma, except t = 3 Ma for Stg. 2 alunite and jarosite)

Table 19. Lead Isotope Ratios for Whole Rocks and Mineral Separates[1]

Sample no.	Rock type[2]	$^{206}Pb/^{204}Pb$	$^{207}Pb/^{204}Pb$	$^{208}Pb/^{204}Pb$
SRTM830	Cinto, ser.	18.817	15.684	38.896
SRM160	Cinto, adv. arg.	18.718	15.664	38.736
87A14	Cinto, ser.	18.890	15.697	39.143
87A180	Cinto, adv. arg.	18.860	15.682	38.934
87A178	Cinto, adv. arg.	18.886	15.701	38.995
87A169	Cinto, adv. arg.	18.878	15.691	38.966
87A316-1	Black chalc.	18.854	15.707	38.998
87A240-1	Black chalc.	18.862	15.690	38.929
87A138	Black chalc.	18.831	15.679	38.908
87A284A	Black chalc.	18.873	15.674	38.901
SRTM595	Cinto, ser.	18.878	15.702	38.998
87A373	Alunite stg. 2	18.878	15.702	38.998
87A380	Alunite stg. 2	18.941	15.708	39.020
87A363	Alunite stg. 2	18.906	15.723	39.090
87A97	Alunite stg. 2	18.902	15.707	39.014
87A237JA	Jarosite	18.884	15.693	38.978

[1] Pb-isotope ratios for unaltered volcanic rocks and galena reported in Arribas and Tosdal (1994)

[2] Abbreviations: Cinto = Cinto ash-flow tuff, ser.= sericitic alteration, adv. arg. = advanced argillic alteration, black chalc. = black chalcedony

Isotopic ratios are present-day measured values, and are not corrected for age. Analytical uncertainty on individual isotopic compositions is <0.05 percent